Natural Products

Deutsche Ausgabe: DOI: 10.1002/ange.201511348
Internationale Ausgabe: DOI: 10.1002/anie.201511348

Chemoreactive Natural Products that Afford Resistance Against Disparate Antibiotics and Toxins

*Lin Du[+], Jianlan You[+], Kenneth M. Nicholas, and Robert H. Cichewicz**

Abstract: *Microorganisms use chemical inactivation strategies to circumvent toxicity caused by many types of antibiotics. Yet in all reported cases, this approach is limited to enzymatically facilitated mechanisms that each target narrow ranges of chemically related scaffolds. The fungus-derived shikimate analogues, pericoxide and pericosine A, were identified as chemoreactive natural products that attenuate the antagonistic effects of several synthetic and naturally derived antifungal agents. Experimental and computational studies suggest that pericoxide and pericosine A readily react via S_N2' mechanisms against a variety of nucleophilic substances under both in vitro aqueous and in situ co-culture conditions. Many of the substitution products from this reaction were highly stable and exhibited diminished toxicities against environmental fungal isolates, including the Tolypocladium sp. strain that produced pericoxide and pericosine A.*

Antibiosis is a type of antagonistic chemical exchange that lies at the heart of many microbe–microbe interactions. The regularity with which genes responsible for biosynthesizing antibiotics/toxins[1] are encountered in genomes, lends support to the idea that natural product "chemical warfare" is a widespread, and perhaps essential feature, of microbial community structure and function.[2] In many cases, direct detection of antibiosis within native microbial communities remains a challenge. However, the biological consequences of these antagonistic interactions, namely antibiotic and toxin resistance mechanisms, are expressed abundantly among both antibiotic producing and non-antibiotic producing bacteria and fungi.[3] The prevalence of antibiotic resistance genes throughout natural microbial populations suggests that antibiosis has long been an evolutionary driver in the refinement and proliferation of antibiotics.

Several types of antibiotic resistance mechanisms are recognized,[4] including 1) membrane impermeabilization, 2) expulsion by efflux, 3) antibiotic inactivation, and 4) modification of cellular targets. Concerning the antibiotic inactivation strategies, all currently known systems share two key features: the processes are enzymatically driven, and the enzymes target narrow ranges of structurally related antibiotics. Herein, we provide evidence for a chemically driven (non-enzymatic) toxin inactivation system employed by a soil ascomycete. This process was serendipitously discovered shortly after we initiated chemical studies of the shikimate-PKS-NRPS metabolite, maximiscin (**1**), which our group identified from *Tolypocladium* sp. Salcha MEA-2 (T1).[5] These results led us to determine that the shikimate portion of **1** is incorporated by a substitution reaction involving a chemoreactive precursor metabolite. This natural product is reactive toward a broad range of exogenous antibiotic/toxic chemicals. Herein, we describe the unique balance of electrophilic promiscuity and chemical stability exhibited by the chemoreactive *Tolypocladium* metabolite and its analogue, and detail how they are likely to protect the fungus from antibiosis.

Before discussing these new discoveries, it should be noted that, during the initial stages of our follow-up studies about the production of **1**, we were confronted with data at odds with our original hypothesis of the metabolite's absolute configuration (details of these studies are provided in the Supporting Information). New results led us to realize that during the original VCD experiments, in which **1** was held for hours in DMSO with warming, the compound had rearranged into a new isomeric species, isomaximiscin (**2**; Figure 1A). Despite this setback the finding was auspicious because, 1) it provided an early clue regarding the remarkable process leading to the formation of **1**, 2) it enabled us to couple the spectroscopically derived absolute configuration results for **1** to data reported for synthetically prepared **3** (Figure 1A),[6] and 3) it led us to develop new investigational tools (that is, ^{13}C isotopic labeling analysis and electronic circular dichroism (ECD) measurements; Figure 1B and Supporting Information). The latter was useful for probing the reactivity spectrum of the precursors of **1** with a range of antibiotics and toxins.

Continuing with our exploration of fungus T1, a notable attribute of its behavior was consistent production of secondary metabolites in response to the presence of co-cultured microbial species.[5] Further studies examining additional fungal co-culture scenarios confirmed the robustness of this response (Supporting Information, Table S17). For example, UPLC-ESIMS^n analysis of a co-culture consisting of T1 and *Penicillium* sp. P1 provided evidence for a new compound that yielded ions at m/z 464.2301 ($[M+H]^+$) and m/z 278.1763 ($[M+H]^+$) (Figures 2E and F). Curiously, the difference between these two major ions (Δ m/z 186.0538) was identical to the neutral loss arising from cleavage of the shikimate analogue moiety, which we detected previously during MS^n analysis of **1** (Figures 2A, C and D). This observation alerted

[*] Dr. L. Du,[+] Dr. J. You,[+] Prof. Dr. K. M. Nicholas, Prof. Dr. R. H. Cichewicz
Department of Chemistry and Biochemistry, Natural Products Discovery Group, and Institute for Natural Products Applications and Research Technologies, University of Oklahoma
Norman, OK 73019-5251 (USA)
E-mail: rhcichewicz@ou.edu
[+] These authors contributed equally to this work.
Supporting information and the ORCID identification number(s) for the author(s) of this article can be found under http://dx.doi.org/10.1002/anie.201511348.

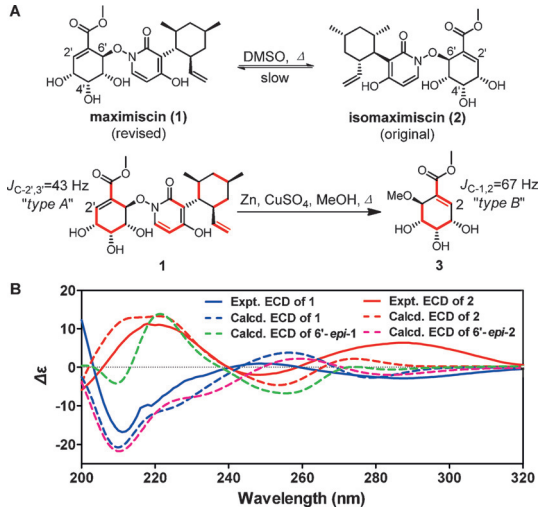

Figure 1. A) Structures for maximiscin (**1**) and its rearrangement artifact, isomaximiscin (**2**). ^{13}C isotope incorporation (accomplished by feeding [U-$^{13}C_6$]-D-glucose to the fungus and analyzing the resulting $^1J_{C\text{-}C}$ coupling values) was used to monitor the origin of the C-2′ position in **1** and the corresponding C-2 position for the key chemical degradation product, pericosine C (**3**). B) Experimental and calculated ECD spectra (TD-DFT) were used to resolve the absolute configurations of **1** and **2**. The illustrated ^{13}C labeling and ECD methods developed during the structure revision process for **1** were instrumental to understanding the structures and mechanisms of formation of compounds described in this study. Details of the rationale applied to structure revision of **1**, along with the experimental methods created for this purpose, are provided in the Supporting Information.

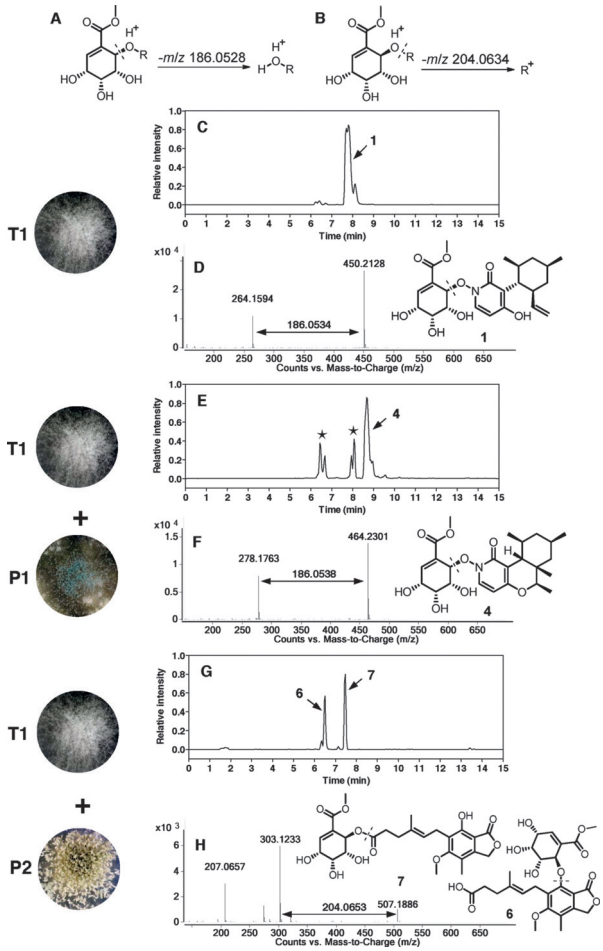

Figure 2. UPLC-ESIMS^n profiling of selected secondary metabolites produced by *Tolypocladium* sp. T1 (C and D) and co-culture of T1 with *Penicillium* sp. P1 (E and F) and P2 (G and H). A) and B) Proposed MS^n splitting patterns for shikimate substitution products. Selected ion traces for *m*/*z* 450.2, 464.2, and 507.2 are shown in (C), (E), and (G), respectively. Their corresponding MS^n spectra are shown in (D), (F), and (H). Figure 2H shows the MS^n spectrum of **6**, which is identical to that of **7**. MS signals of unknown substances (⋆).

us to the possibility that the new co-culture metabolite might also contain a shikimate analogue moiety. Scale-up preparation, purification, and structure determination revealed that the new compound was structurally related to **1** and was subsequently named pseudomaximiscin A (**4**; Figure 2F). Similar to **1**, incubation of **4** in [D_6]DMSO led to its isomerization, resulting in an approximately 1:1 equilibrium mixture with its diastereomeric product, pseudomaximiscin B (**5**; Figure 3).

Intrigued by the discovery of **4**, we re-examined the MS^n data from the fungal co-culture experiments and noted that, besides the recurring Δ *m*/*z* 186 loss corresponding to several new metabolites, a second neutral loss of *m*/*z* 204 (Figure 2B) was apparent. Using these two parameters to filter the MS^n data, a neutral loss event of *m*/*z* 204 was identified for two metabolites that were generated when fungus T1 was co-cultured with *Penicillium* P2 (Figure 2G and H). Scale-up production yielded the new compounds, mycophenolic acid 3-*O*-pericosine (**6**) and mycophenolic acid 16-*O*-pericosine (**7**). While **6** was optically active ($[\alpha]_D^{20}$ −126), **7** was not, indicating that it was a racemic mixture. Deliberate probing of all samples by UPLC-ESIMS^n and ion-selective MS revealed that the likely non-shikimate precursor metabolites of **4**, **6**, and **7** came from the co-culture partners (Figure 3). For example, fungus P1, was deduced to be the source of metabolite PF1140 (**8**),[7] whereas fungus P2 made mycophenolic acid (**9**).[8] Therefore, compounds **4**, **6**, and **7** were proposed to be chimeric metabolites made from the union of **8** or **9** with an as yet undetermined chemoreactive compound from fungus T1.

To determine how the T1 culture facilitated this process, an experiment was conceived using P1-derived metabolite **8** as "bait" in a chemoassay-guided process meant to uncover the origins of the shikimate analogue incorporation (Scheme 1). Initially, purified **8** was mixed with dialysate prepared from one-week-old T1 culture broth. LAESIMS monitoring of the reaction revealed that compound **4**, which yielded a $[M+H]^+$ quasi molecular ion peak at *m*/*z* 464.2301, was detectable with dialysate prepared with both large (1000 kDa) and small (0.5–1 kDa) average molecular weight cutoff membranes. This suggested that the reaction could occur in a cell-free environment by means of a non-enzymatic process. Subsequently, T1 cultures were successively extracted with EtOAc and *n*-butanol. While the remaining aqueous layer was inactive, samples from both organic layers generated **4** upon addition of **8**. Chemoassay-directed HPLC fractionation enabled purification of two shikamate ana-

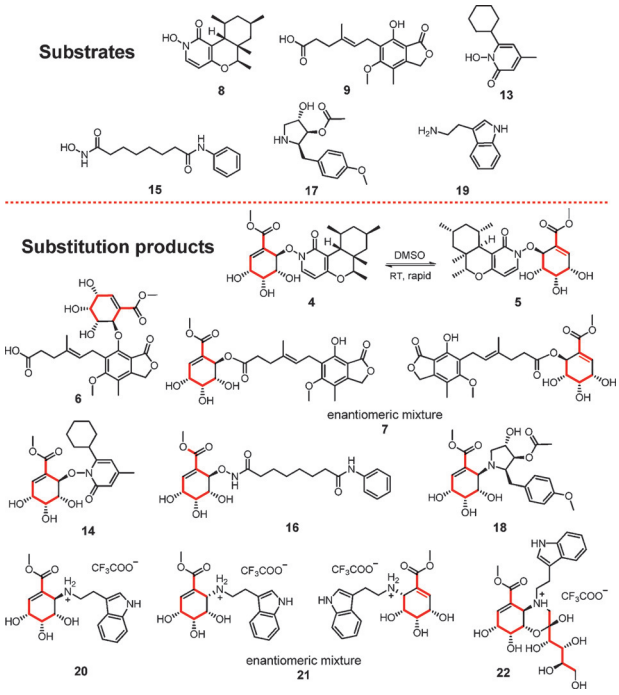

Figure 3. Substrate transformation products obtained from *Tolypocladium* sp. T1. The ^{13}C-labeling patterns for the substrate-shikimate substitution products were generated by feeding T1 with [U-$^{13}C_6$]-D-glucose.

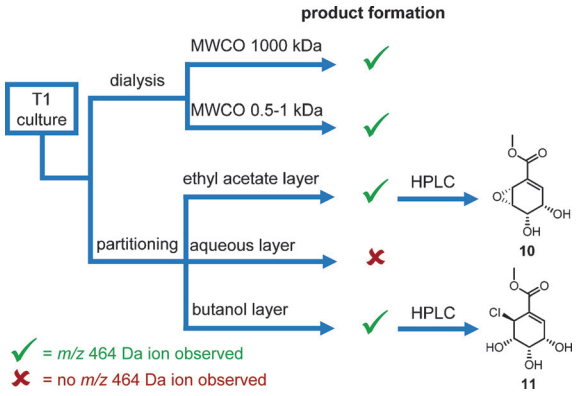

Scheme 1. Chemoassay-guided identification of shikimate analogues **10** and **11**. The culture broth of T1 was subjected separately to dialysis and partitioning, and treated with the P1-derived metabolite **8**. LAESIMS was used to track the presence of **10** and **11** by monitoring the formation of **4** (*m*/*z* 464 Da).

logues; the new epoxide metabolite pericoxide (**10**) from the EtOAc extract, and the known chlorinated compound (+)-pericosine A (**11**)[6] from the *n*-butanol extract. These results led us to determine that **10** and **11** were the probable precursors to the non-enzymatic formation of **1** in T1 cultures, rather than the 6-OH analogue we previously implicated.[5]

With **10** and **11** identified as candidates for the formation of the co-cultured-derived hybrid metabolites, the chain of antecedence linking the two compounds was called into question. UPLC-ESIMS^n analysis of the MeOH extract of the cell lysate of T1 revealed that neither **10**, **11**, nor any other hybrid metabolites (**1** for example) were detectable intracellularly, implying that both **10** and **11** were either formed extracellularly, or sequestered and secreted from the cells upon their formation. By further examination of the ^{13}C-labeled forms of **10** and **11** (prepared by feeding fungus T1 [U-$^{13}C_6$]-D-glucose), it was determined that both compounds were present in the spent culture broth as single enantiomers exhibiting a "type B" ^{13}C-labeling pattern (Figure 1A and Supporting Information). Treatment of ^{13}C-labeled **10** with NaCl in double-distilled water yielded **11**, seemingly via an S_N2 mechanism (Figure 4A). ECD analysis showed that **11**

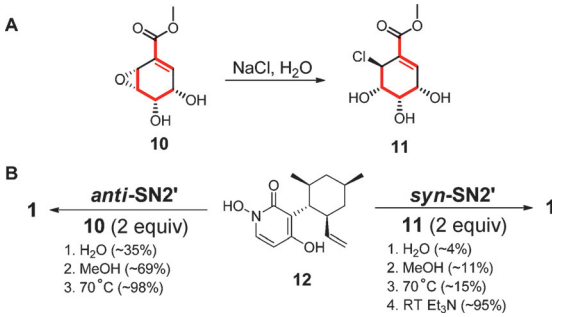

Figure 4. Electrophilic natural products from fungus T1. A) ^{13}C-labeling patterns for **10** and **11** generated by feeding T1 [U-$^{13}C_6$]-D-glucose with NaCl present in the culture medium. B) Selectivity and yields (%) for the S_N2' coupling of **12** with **10** and **11**. The reaction rates of selected model substrates (**13** and **17**) were tested (Supporting Information, Figure S127).

prepared from **10**, as well as directly from the fungal culture broth, bore the same absolute configuration (Supporting Information, Figure S126). These results imply that **11** was non-enzymatically produced from **10** within the T1 culture. This hypothesis was tested by preparing fungal culture broth for T1 using Millipore water and observing that the yield of **11** was strongly correlated with the quantity of NaCl or other Cl^- sources that were added to the culture medium (Supporting Information, Figure S124). Though the origin of **10** remains undetermined, a hint of the process involved in its formation can likely be gleaned from the biosynthesis of the chorismic acid derivative, cyathiformine A,[9] (Supporting Information, Figure S130).

The roles that **10** and **11** might play in the production of **1** were tested by assessing their reactivities toward pyridoxatin (**12**).[5] Production of **1** was found to occur in Millipore water upon addition of **12** to both **10** and **11**. Manipulation of selected reaction conditions (solvent, temperature, and catalyst) confirmed that epoxide **10** was generally more reactive toward **12** than its halohydrin counterpart **11**. In all cases enantiomerically pure **1** was obtained as the product, indicating that a selective S_N2' mechanism was involved in the formation of **1** under both synthetic and in situ culture conditions (Figure 4B).

To test the promiscuous reactivity of **10** and **11** toward other compounds, T1 cultures were treated with a panel of substrates that included chemically diverse functional groups: hydroxamic acids, phenols, carboxylic acids, alcohols, alkenes,

amides, and amines (Supporting Information, Table S14). Candidate products from each reaction were purified and their structures confirmed by HRESIMS and multidimensional NMR spectroscopy. Additionally, T1 cultures were supplied with [U-$^{13}C_6$]-D-glucose so that the labeling patterns of the resulting products (Figure 3) would afford insights regarding the probable substitution mechanisms involved in their formation (that is, S_N1, S_N2, or S_N2'; Supporting Information, Figure S125). Additionally, the absolute configuration of the C-6′ position in each product was determined by comparing its experimental and theoretical ECD data (Supporting Information, Figure S126). Based on these analyses, the stereoselectivities of the coupling reactions (particularly *anti*- versus *syn*-S_N2' mechanisms) were systematically assessed (details of the structure determination for the new compounds are provided in the Supporting Information, Figure S125).

The results demonstrated that **10** and **11** were decidedly reactive toward diverse chemical targets. Stereoselective S_N2' (*anti*-S_N2' for **10** and *syn*-S_N2' for **11**) reaction processes were observed involving all the hydroxamic acids, including PF1140 (**8**), ciclopirox (**13**), and SAHA (**15**), to give optically active products **4**, **14**, and **16**, respectively. A similar S_N2' reactivity pattern was observed involving reaction of **10** and **11** with phenol-containing (3-OH of **9**) and secondary amine-containing (anisomycin (**17**)) substrates. In contrast, reaction with the carboxylic acid moiety of **9** yielded racemic **7** (Supporting Information, Figure S26). The 5′*R**6′*R** relative configuration of the product was assigned based on an examination of its ^{13}C NMR chemical shifts in comparison with DFT calculated data (Supporting Information, Figures S12–S14). Whether product mixture **7** arose from competing reaction processes or a rearrangement remains unknown.

The primary amine tryptamine (**19**) was also administered to T1, resulting in formation of products **20** and **21**, and an unexpected novel product named mallimiscin (**22**; Figure 3). Distinct $J_{H\text{-}5',H\text{-}6'}$ values aided determination of the 5′,6′-relative configuration of the products (*trans* greater than 9 Hz, *cis* ca. 5 Hz). Whereas **20** was obtained as an enantiomerically pure product, diastereomers of **21** were obtained as a racemate (Supporting Information, Figure S27). Compound **22** was seemingly formed by a Maillard reaction of **20** with D-glucose, based on its ^{13}C-labeling pattern, ROESY correlations, $J_{H,H}$ coupling constants, and ECD calculation (Figures 3; Supporting Information, Figures S126 and S127).

To better understand the selectivity exhibited by **10** and **11** for several of the substrates, DFT calculations were employed to determine the energies of the transition states for *syn*-S_N2', *anti*-S_N2', and S_N2 reactions of **10** and **11** with the model hydroxamic acid **23**. The β-hydroxycarbonyl hydroxy group in **23** was estimated to have a pK_a of about 7–9, indicating that its anionic form may be present as the reactive nucleophile in aqueous media. The computational results (Figure 5) were in quantitative agreement with the experimentally observed regio- and stereoselectivities of reactions between hydroxamic acids and both **10** and **11**. For the reaction of **23** with **11**, the *syn*-S_N2' transition state (and its corresponding activation energy) was the lowest in energy by a substantial margin. In

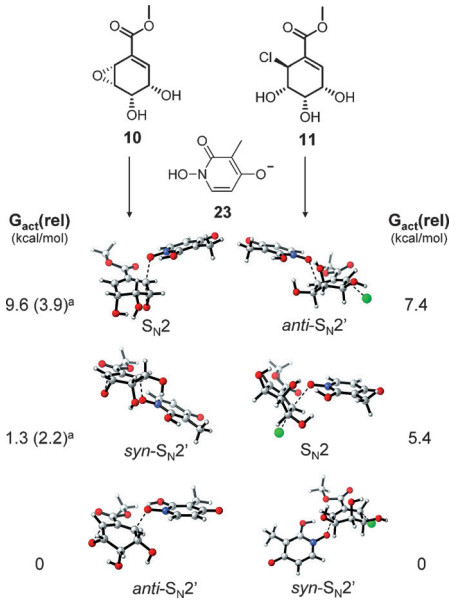

Figure 5. Calculated transition states and relative free energies of activation for the reactions of **10** and **11** with 1-hydroxy-3-methyl-2-oxo-1,2-dihydropyridin-4-olate (**23**). [a]B3LYP/6-31G(d) basis sets were used to determine transition state structures; free energies were obtained from single point calculations by M06-2X and MP2 (in parenthesis) methods and a 6-311++G(d,p) basis set.

contrast, the *anti*-S_N2' pathway was favored by a smaller margin in the reaction involving epoxide **10** (depending on the computational method employed). Notably, each of the transition states identified in these calculations suggest that tautomerization occurs between the C-2 carbonyl and *N*-OH groups.

The observed (and calculated) exclusively *syn*-S_N2' (for allyl-X) or *anti*-S_N2' (for vinyl oxirane) selectivity detected among some of these reactions has been found in other vinylogous nucleophilic substitution reaction systems. However, depending on the substrate, nucleophile, and solvent employed, there are also many exceptions.[10] Numerous factors have been invoked to explain the observed selectivity in such reactions, including frontier orbital and coulombic interactions, conformational and steric effects, specific Lewis acid–base and H-bonding interactions, and solvation. The origin of the remarkable and divergent stereoselectivities in the reactions of these two allylic substrates is presently unclear and its elucidation will require additional experimental and computational investigation.

Reflecting on the potential biological roles of electrophilic **10** and **11**, we noted that the natural product precursors made by T1's partner fungus possessed antifungal activities. This prompted us to question what effect the addition of the shikimate analogue moiety had on the bioactivities of compounds **8**, **9**, **12**, and the other nucleophilic substances that we tested. A panel of fungi, including four *Tolypocladium* spp. (T1–T4), four *Penicillium* spp. (P1–P4), and *Aspergillus niger* (A1), were selected for assessment. The test revealed a distinct trend in which the antifungal activities of the substrates were greatly diminished or abolished following addition of the shikimate analogue moiety (Figure 6A). For

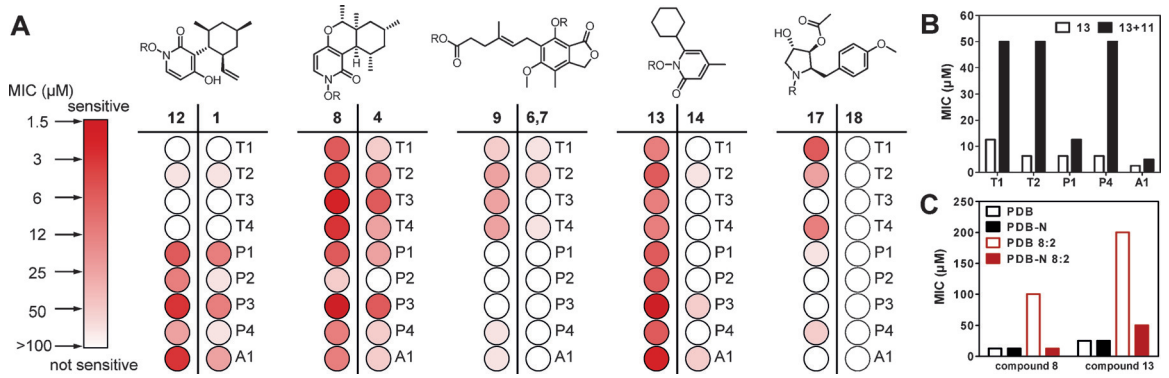

Figure 6. A) Comparison of the antifungal efficacy of the shikimate-substrate substitution products (**1**, **4**, **6**, **7**, **14**, and **18**) and their corresponding parent compounds (**8**, **9**, **12**, **13**, and **17**) against a panel of test fungi (T1-T4, P1-P4, and A1). B) Co-treatment of fungi with **11** and **13** (fungi T1, T2, P1, P4, and A1) reduced the antifungal efficacy of **13**. C) Effect of supplemental $NaNO_3$ in the test medium on the antifungal efficacy of **8** and **13** against T1. Media types: potato dextrose broth (PDB), PDB plus 2 g L^{-1} $NaNO_3$ (PDB-N), a mixture of a centrifuged broth of T1 grown in PDB for 5 days with fresh PDB in a ratio of 8:2 (PDB 8:2), and a mixture of a centrifuged broth of T1 grown in PDB-N for 5 days with fresh PDB in a ratio of 8:2 (PDB-N 8:2).

example, both the P1-derived antifungal agent **8** and the synthetic antifungal agent **13** showed growth inhibition against all of the fungal strains, with minimum inhibitory concentration (MIC) values in the range of 1–50 μM. By comparison, adducts **4** and **14** exhibited a greater than five-fold decrease in potencies on average. To test the capacity of **11** to block the toxicity of **13** in real time, fungal cultures were preincubated with **11** and then treated with varying doses of **13**. This regimen of preadministering **11** afforded an up to eight-fold decrease in the MIC of **13** (Figure 6B). Our prior time-course studies, which examined production of **10** and **11**, showed that these metabolites rapidly accumulated in T1 cultures after 96 hours. We had also noted that the addition of $NaNO_3$ to the culture medium thoroughly abolished the formation of **10** and **11**. Using this information, we determined that fungus T1 was equally sensitive to the antifungal activities of **8** or **13** in both freshly prepared normal and $NaNO_3$-supplemented media during a three-day test window. However, when five-day-old T1 culture broth was used to prepare the test medium, the non-$NaNO_3$-supplemented T1 culture became increasingly resistant to **8** and **13** (Figure 6C).

In summary, these studies provide evidence for a new chemically facilitated mode of toxin resistance exhibited by a soil ascomycete. Whereas previously reported resistance mechanisms involving antibiotic modification depended on the enzymatic modification of target substrates, fungal metabolites **10** and **11** functioned as electrophilic warheads that were reactive to a wide variety of natural and synthetic organic substances. The actions of these metabolites appear to limit the deleterious effects of antibiotics/toxins against their microbial targets. Further studies investigating the steric and stereoelectronic regulation of this process are expected to inspire the creation of new biologically compatible toxin scavenging materials.

Acknowledgements

We appreciate the thought-provoking comments offered by Dr. Jason Clement and Dr. Will Gutekunst concerning reaction mechanisms. We also thank Prof. Dr. Peng Liu (U. Pittsburgh) for helpful discussions regarding the computational modeling. This work was funded in part by grants from the National Institute of General Medical Sciences (R01GM107490) and National Institute of Allergy and Infectious Diseases (R01AI085161) of the National Institutes of Health (R.H.C.).

Keywords: antibiotic resistance · co-culture · fungi · isotope labeling · natural products · substitution reactions

How to cite: *Angew. Chem. Int. Ed.* **2016**, *55*, 4220–4225
Angew. Chem. **2016**, *128*, 4292–4297

[1] Z. Charlop-Powers, J. G. Owen, B. V. B. Reddy, M. A. Ternei, S. F. Brady, *Proc. Natl. Acad. Sci. USA* **2014**, *111*, 3757–3762.
[2] a) L. L. Kinkel, D. C. Schlatter, K. Xiao, A. D. Baines, *ISME J.* **2014**, *8*, 249–256; b) O. X. Cordero, H. Wildschutte, B. Kirkup, S. Proehl, L. Ngo, F. Hussain, F. Le Roux, T. Mincer, M. F. Polz, *Science* **2012**, *337*, 1228–1231; c) T. L. Czaran, R. F. Hoekstra, L. Pagie, *Proc. Natl. Acad. Sci. USA* **2002**, *99*, 786–790; d) M. F. Weber, G. Poxleitner, E. Hebisch, E. Frey, M. Opitz, *J. R. Soc. Interface* **2014**, *11*, 20140172; e) M. I. Abrudan, F. Smakman, A. J. Grimbergen, S. Westhoff, E. L. Miller, G. P. van Wezel, D. E. Rozen, *Proc. Natl. Acad. Sci. USA* **2015**, *112*, 11054–11059.
[3] a) M. K. Gibson, K. J. Forsberg, G. Dantas, *ISME J.* **2015**, *9*, 207–216; b) E. C. Pehrsson, K. J. Forsberg, M. K. Gibson, S. Ahmadi, G. Dantas, *Front. Microbiol.* **2013**, *4*, 00145.
[4] J. M. A. Blair, M. A. Webber, A. J. Baylay, D. O. Ogbolu, L. J. V. Piddock, *Nat. Rev. Microbiol.* **2015**, *13*, 42–51.
[5] L. Du, A. J. Robles, J. B. King, D. R. Powell, A. N. Miller, S. L. Mooberry, R. H. Cichewicz, *Angew. Chem. Int. Ed.* **2014**, *53*, 804–809; *Angew. Chem.* **2014**, *126*, 823–828.
[6] a) Y. Usami, M. Ohsugi, K. Mizuki, H. Ichikawa, M. Arimoto, *Org. Lett.* **2009**, *11*, 2699–2701; b) D. R. Boyd, N. D. Sharma,

C. A. Acaru, J. F. Malone, C. R. O'Dowd, C. C. Allen, P. J. Stevenson, *Org. Lett.* **2010**, *12*, 2206 – 2209.
[7] E. D. de Silva, A. S. Geiermann, M. I. Mitova, P. Kuegler, J. W. Blunt, A. L. Cole, M. H. Munro, *J. Nat. Prod.* **2009**, *72*, 477 – 479.
[8] X. Lu, Z. Zheng, H. Zhang, C. Huo, Y. Dong, Y. Ma, X. Ren, A. Ke, J. He, Y. Gu, Q. Shi, *J. Antibiot.* **2009**, *62*, 527 – 529.
[9] A. Arnone, R. Cardillo, G. Nasini, O. Vajna de Pava, *Tetrahedron* **1993**, *49*, 7251 – 7258.
[10] a) D. Sinou, *Organic Reactions in Water: Principles, Strategies and Applications* (Ed.: U. M. Lindström), Wiley-Blackwell, Oxford, **2007**, pp. 236 – 255; b) A. Chanda, V. V. Fokin, *Chem. Rev.* **2009**, *109*, 725 – 748; c) P. E. Savage, *Chem. Rev.* **1999**, *99*, 603 – 621.

Received: December 7, 2015
Revised: January 18, 2016
Published online: March 1, 2016

